Experimental Studies on Effects of Nozzle Size and Jet Reynolds Number on Impingement Heat Transfer with Axisymmetric Water Jets

Nirmal Kumar Kund
Department of Production Engineering
Associate Professor,Veer Surendra Sai University of Technology, Burla, Odisha, India

Abstract-*This paper presents the experimental studies on the heat transfer behavior of an axisymmetric water jet impinging on a heated plate. Various influencing parameters pertaining to the thermal performance of the water jet impingement are identified and their effects on heat transfer characteristics are also investigated. The parameters taken into account are nozzle diameter (3-6 mm) and jet Reynolds number (800-3200). Additionally, the studies are limited to a constant heat flux situation. The careful observations of the results reveal that the performance of water jet can be optimized with regard to these key parameters. However, with the current experimental conditions, the nozzle diameter of 5 mm with the jet Reynolds number of 2400 gives moderate heat transfer characteristics and is the optimum.*

Keywords-Water jet, Target plate, Nozzle diameter, Jet Reynolds number.

I. INTRODUCTION

The ever growing needs for faster and smaller electronic components in the electronic industry has resulted in the development of compact electronic equipments with high power densities. Conventional air cooling is insufficient in most cases to help sustain and safeguard the electronics components from the thermal failure. Garimella and Nenaydykh [1] have experimentally investigated the effect of nozzle geometry on the local heat transfer of FC-77 *per-fluorinated dielectric* liquid for normal jet impingement. Roy et al. [2] studied both experimentally and numerically heat transfer of an inclined surface subject to an impinging airflow. Chakraborty and Dutta [3] found analytical solutions for heat transfer during cyclic melting and freezing of a phase change material used in electronic and electrical packaging. Lee et al. [4] have examined the effects of nozzle diameter on impinging jet heat transfer and fluid flow. Nayak et al. [5] developed a numerical model for heat sinks with phase change materials and thermal conductivity enhancers. Eren and Celik [6] investigated the heat transfer characteristic of a heated flat plate by an obliquely impinging air jet. Pavlova and Amitay [7] studied on the heat transfer behavior of electronics with synthetic normal Jet Impingement.

II. LITERATURE REVIEW

Furthermore, Agostini et al. [8] illustrated the state of art of the high heat flux cooling technologies. Adoni et al. [9] developed a thermo-hydraulic model for capillary pumped loop and loop heat pipe used for cooling of electronics. Behera et al. [10] investigated numerically on the heat transfer of interrupted impinging air jets used for electronics cooling. Saha et al. [11] investigated on optimum distribution of fins in heat sinks filled with phase change materials. Sagot et al. [12] studied the jet impingement heat transfer on a flat plate at a constant wall temperature by using gas jets. Sanyal et al. [13] numerically studied on heat transfer from pin-fin heat sink using steady and pulsated impinging air jets. Saha and Dutta [14] developed heat transfer correlations for PCM-based heat sinks with plate fins. Chaudhari et al. [15] examined heat transfer characteristics of synthetic air jet impingement cooling. Narasimhan et al. [16] investigated on thermal management using the bi-disperse porous medium approach. Yu et al. [17] compared a series of double chamber model with various hole angles for enhancing cooling effectiveness by air jets. Besides, Yu et al. [18] also carried out numerical simulation on the effect of turbulence models on impingement cooling of double chamber model. Cheng et al. [19] numerically studied air/mist impinging jets cooling effectiveness under various curvature models. Nguyen et al. [20] investigated cooling effect by sub-zero cold air jet in the grinding of a cylindrical component. Gould et al. [21] studied jet impingement cooling of a silicon carbide module. Zhao et al. [22] also investigated the effect of guide wall on jet impingement cooling.

III. OBJECTIVES OF PRESENT RESEARCH WORK

Careful review and examination of the already stated relevant literature reveals no clear cut and prior theoretical and experimental investigation on the local heat transfer under an obliquely impinging, axisymmetric free surface water jet flow for Reynolds number of range 800-3200. In addition, to the best of the authors' knowledge, there is not a single comprehensive experimental study pertaining to the effects of the jet velocity rate and the nozzle diameter on the heat transfer behavior over the heated target plate previously maintained at a uniform heat flux of 6.25 W/cm2 for investigating the relative importance of the key parameters involved. With this viewpoint, the current paper demonstrates experimental investigations relating to the influence and role of the jet Reynolds number (800-3200) and the jet diameter (3-6 mm) on the local heat transfer characteristics over a flat plate heated from the underneath and maintained at a uniform flux of 6.25 W/cm2, for free surface axisymmetric water jet impingements. Additionally, the results thus obtained are analyzed and compared, so as to realize deeply, the heat transfer behavior over the target plate for achieving better cooling effect.

IV. TEST APPARATUS AND METHOD

It enumerates about the details of a series of rigorous and numerous experiments on jet impingement cooling starting from the descriptions of various components of the experimental setup to the smooth control/regulation of different key parameters (such as jet flow rate, input voltage and current to the heater, nozzle to target plate spacing and nozzle inclination) involved in affecting the heat transfer during the jet impingement. The basic attempt of this work is to measure the equilibrium temperatures (corresponding to the steady state condition) at different points on the target plate subjected to constant heat flux during the jet impingement at uniform rate, while setting the stated parameters at appropriately suitable and predetermined values.

A. Description of the physical problem

In order to achieve the said objective, the model is selected accordingly and the schematic sketch of the physical model is illustrated in Fig. 1.

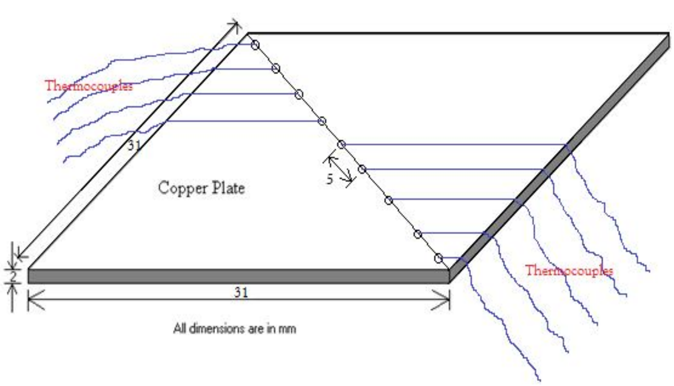

Fig. 1. Schematic sketch of the physical model

The physical problem consists of a copper plate (also termed as target plate) of dimensions 31×31×2 mm on which T-type thermocouples are mounted along one of the diagonal lines with spacing of 5 mm between two consecutive thermocouples. This target plate is mounted on a heater, whereas, these thermocouples are connected to a data acquisition system to record temperature data continuously while conducting experiments. The temperature variation on the plate is assumed to be a step function. The assumption is only used for calculating the average heat transfer coefficient or the average Nusselt number for the normal jet impingement.

Here, local heat transfer coefficient,

$$h_i = \frac{Q_{out}}{A_h(T_{si} - T_j)}\ ;\ Q_{out} = VI \tag{1}$$

So, average heat transfer coefficient, $\bar{h} = \frac{\sum h_i A_i}{\sum A_i}$

(2)

Average heat transfer coefficient,

$$\bar{h} = \left[\frac{Q_{out}}{A_h^2}\right]\sum\left(\frac{A_i}{T_{si} - T_j}\right) \tag{3}$$

Hence, local Nusselt number, $Nu_i = \frac{h_i d}{k}$

(4)

Now, average Nusselt number, $\overline{Nu} = \frac{\bar{h} d}{k}$

(5)

B. Description of the experimental setup

Fig. 2 represents the photograph of the complete assembly of the experimental setup. It consists of a heater kept in a rectangular Plexiglas box, a nozzle connected to a rotameter via a flexible pipe and a copper target plate mounted on the heater. The heater consisting of tungsten filament (with heater wire diameter of 0.576 mm and heater element resistance of 4.3 Ω) is connected to a dual supply D.C. power source. For particular values of current and voltage the heat flux to the heater remains constant. A digital multimeter (Keithley 2700 model) is used to measure the voltage, whereas, current is directly measured from the display unit of power supply. The rotameter is connected to a water supply tap by means of a flexible pipe with brass ball valve arrangement for regulating water flow. The copper plate mounted on the heater have got grooves underside in order to accommodate thermocouples connected to data acquisition system. The surface of the copper plate is polished with sand paper and then is cleaned with acetone before conducting experiments. The nozzle is kept perpendicular or inclined to the target plate by means of a vertical stand with clamp arrangement. The test fluid (water) discharges out through the outlet of the test chamber after impinging on the target plate.

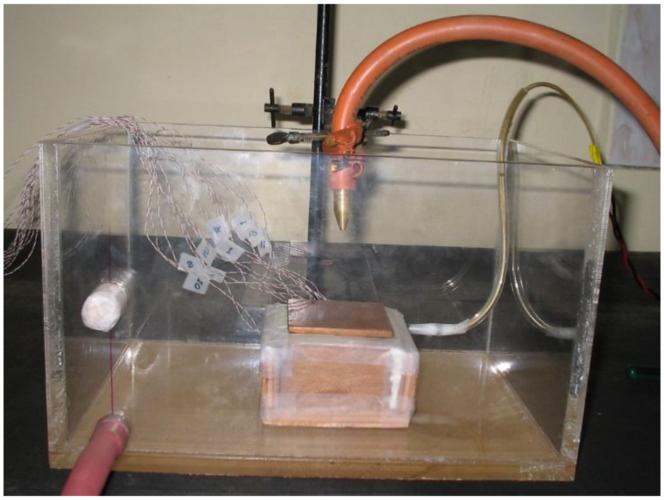

Fig. 2. Photograph of the experimental setup

C. Experimental procedure

It involves the measurements of following key process parameters.

1. *Measurements of nozzle to target plate spacing and nozzle inclination*

Basically, the nozzle is fitted to a clamp attached to the vertical stand whereas the target plate is mounted on the heater. Hence, the distance between nozzle and target plate spacing (Z) is measured by means of filler gauges. The nozzle inclination (θ) with respect to horizontal target plate is checked and adjusted by using a protractor attached to the clamp.

2. *Flow measurement*

During the jet impingement the flow rate of water in the tube connecting the tap to the nozzle is measured by means of a rotameter (having measuring range of 0-120 lph). The measurement uncertainty of rotameter is ±0.01 times the flow rate in lph. In order to avoid fluctuations and to get the desired flow rate of water, the fine tuning of rotameter is also done. The average jet velocity exiting the nozzle is calculated from the jet flow rate. And also, the corresponding jet Reynolds number is calculated from this jet velocity.

3. *Temperature measurement*

Here, as mentioned in Table 1, polytetrafluoroethylene (PTFE) coated T-type (Copper- Constantan, manufactured by T C Ltd, UK) thermocouples (of diameter 0.205 mm with measuring range of 0-200° C) are used to measure temperature at different locations on the target plate during the impingement of water jet. These thermocouples are calibrated well against a platinum resistance thermometer. A Julabo FH40-MH circulation bath is used for this purpose. As per the manufacturer's specification of thermocouples, the response time is 0.8 s and the measurement uncertainty is ±0.004T, where T is the measured temperature in degrees Celsius. As already mentioned, these temperature data are periodically recorded by an interface computer through a data acquisition system. The data acquisition system consists of a 40-channel Keithley thermocouple plug-in card with "T" type 30-gauge Teflon coated copper-constantan thermocouples monitoring the thermal evolution.

Table 1

Specifications of thermocouples

Material	Class	Size (mm)	Range (°C)
Copper-Constantan	PTFE coated T-type	0.205	0-200°C

V. RESULTS AND DISCUSSION

Rigorous experiments are performed to study the effects of both nozzle diameter (d) and jet Reynolds number (Re) on the heat transfer behavior over the heated target plate subjected to a uniform heat flux. At the outset, a base case of nozzle diameter 5 mm and a normal water jet of flow rate 30 lph corresponding to Reynolds number of 2400 is considered. The heat flux of 6.25 W/cm2 (corresponding to 30 V and 2 A of D. C. power source associated with copper target plate of size 31 mm × 31 mm) is applied in all investigations. The results thus obtained in line with the stated base case experimental conditions are analyzed to investigate further the role and effect of the said key process parameters involved.

A. EFFECT OF NOZZLE DIAMETER

Apart from the stated base case involving nozzle diameter of 5 mm, in this study three more nozzle diameters of 3, 4 and 6 mm are taken into account with the said experimental conditions. The results thus obtained are compared to investigate the role and effect of the nozzle diameter. Figs. 3-5 illustrate the variation of both stagnation and average Nusselt numbers with the nozzle diameter.

Fig. 3 shows the variation of both stagnation and average Nusselt numbers with the nozzle diameter for four different jet Reynolds numbers of 800, 1600, 2400 and 3200. With the jet Reynolds number of 800, the stagnation Nusselt numbers are 45, 36, 30 and 27 besides the average Nusselt numbers of 37, 29, 25 and 23 for the nozzle diameters of 3, 4, 5 and 6 mm, respectively. Likewise, with the jet Reynolds number of 1600, the stagnation Nusselt numbers are 61, 50, 43 and 38 besides the average Nusselt numbers of 45, 37, 33 and 29 for the nozzle diameters of 3, 4, 5 and 6 mm, respectively. Similarly, with the jet Reynolds number of 2400, the stagnation Nusselt numbers are 73, 60, 51 and 45 besides the average Nusselt numbers of 51, 42, 37 and 32 for the nozzle diameters of 3, 4, 5 and 6 mm, respectively. Furthermore, with the jet Reynolds number of 3200, the stagnation Nusselt numbers are 86, 71, 60 and 52 besides the average Nusselt numbers of 58, 48, 42 and 36 for the nozzle diameters of 3, 4, 5 and 6 mm, respectively.

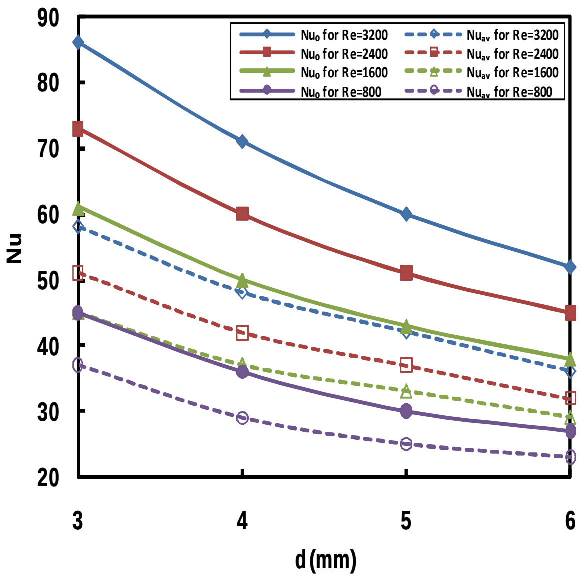

Fig. 3. Variation of Nusselt number with nozzle diameter at four different jet Reynolds numbers

Fig. 4 shows the variation of both stagnation and average Nusselt numbers with the nozzle diameter for four different nozzle to plate spacings of 4, 5, 6 and 7 (times the nozzle diameter). With the nozzle to plate spacing of 4, the stagnation Nusselt numbers are 89, 74, 64 and 55 besides the average Nusselt numbers of 65, 55, 48 and 42 for the nozzle diameters of 3, 4, 5 and 6 mm, respectively. Likewise, with the nozzle to plate spacing of 5, the stagnation Nusselt numbers are 73, 60, 51 and 45 besides the average Nusselt numbers of 51, 42, 37 and 32 for the nozzle diameters of 3, 4, 5 and 6 mm, respectively. Similarly, with the nozzle to plate spacing of 6, the stagnation Nusselt numbers are 61, 50, 43 and 38 besides the average Nusselt numbers of 44, 36, 32 and 27 for the nozzle diameters of 3, 4, 5 and 6 mm, respectively. Furthermore, with the nozzle to plate spacing of 7, the stagnation Nusselt numbers are 53, 43, 37 and 33 besides the average Nusselt numbers of 37, 30, 27 and 22 for the nozzle diameters of 3, 4, 5 and 6 mm, respectively.

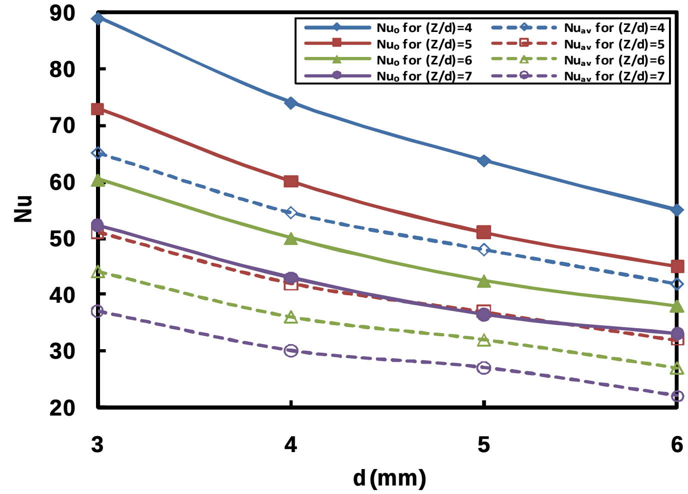

Fig. 4. Variation of Nusselt number with nozzle diameter at four different nozzle to plate spacings

Fig. 5 shows the variation of both stagnation and average Nusselt numbers with the nozzle diameter for five different jet inclinations of 30□, 45□, 60□, 75□ and 90□. With the jet inclination of 30□, the stagnation Nusselt numbers are 115, 98, 85 and 75 besides the average Nusselt numbers of 82, 69, 60 and 51 for the nozzle diameters of 3, 4, 5 and 6 mm, respectively. Likewise, with the jet inclination of 45□, the stagnation Nusselt numbers are 101, 85, 73 and 64 besides the average Nusselt numbers of 72, 60, 52 and 44 for the nozzle diameters of 3, 4, 5 and 6 mm, respectively. Similarly, with the jet inclination of 60□, the stagnation Nusselt numbers are 90, 75, 64 and 56 besides the average Nusselt numbers of 63, 52, 45 and 38 for the nozzle diameters of 3, 4, 5 and 6 mm, respectively. Furthermore, with the jet inclination of 75□, the stagnation Nusselt numbers are 81, 67, 57 and 50 besides the average Nusselt numbers of 56, 46, 40 and 34 for the nozzle diameters of 3, 4, 5 and 6 mm, respectively. Additionally, with the jet inclination of 90□, the stagnation Nusselt numbers are 73, 60, 51 and 45 besides the average Nusselt numbers of 51, 42, 37 and 32 for the nozzle diameters of 3, 4, 5 and 6 mm, respectively.

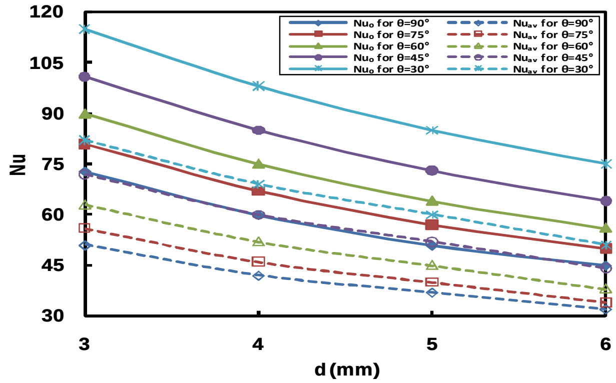

Fig. 5. Variation of Nusselt number with nozzle diameter at five different jet inclinations

From the quoted figures, it is quite obvious that both stagnation and average Nusselt numbers decrease with increase in nozzle diameter. This can be owing to the fact that for same jet flow rate the higher nozzle diameter causes the lower jet velocity/jet Reynolds number and hence gives rise to the carrying away of heat from the target plate at relatively slower rate. In addition, for a particular nozzle diameter, both stagnation and average Nusselt numbers increase with Reynolds number (Fig. 3). Similarly, for a particular nozzle diameter, both stagnation and average Nusselt numbers decrease with increase in Reynolds number/jet inclination (Fig. 4 and Fig. 5). And also, from Figs. 3-5, it is evident that the variation of both stagnation and average Nusselt numbers with nozzle diameter is almost linear.

B. EFFECT OF JET REYNOLDS NUMBER

Besides the said base case involving jet Reynolds number of 2400, in the present investigation three more jet Reynolds numbers of 800, 1600 and 3200 are considered with the stated experimental conditions. The corresponding results are analyzed and compared to study the role and effect of the jet Reynolds number. Figs. 6-8 show the variation of both stagnation and average Nusselt numbers with the Reynolds number.

Fig. 6 shows the variation of both stagnation and average Nusselt numbers with the Reynolds number for four different nozzle diameters of 3, 4, 5 and 6 mm. With the nozzle diameter of 3 mm, the stagnation Nusselt numbers are 45, 61, 73 and 86 besides the average Nusselt numbers of 37, 45, 51 and 58 for the jet Reynolds numbers of 800, 1600, 2400 and 3200, respectively. Likewise, with the nozzle diameter of 4 mm, the stagnation Nusselt numbers are 36, 50, 60 and 71 besides the average Nusselt numbers of 29, 37, 42 and 48 for the jet Reynolds numbers of 800, 1600, 2400 and 3200, respectively. Similarly, with the nozzle diameter of 5 mm, the stagnation Nusselt numbers are 30, 43, 51 and 60 besides the average Nusselt numbers of 25, 33, 37 and 42 for the jet Reynolds numbers of 800, 1600, 2400 and 3200, respectively. Furthermore, with the nozzle diameter of 6 mm, the stagnation Nusselt numbers are 27, 38, 45 and 52 besides the average Nusselt numbers of 23, 29, 32 and 36 for the jet Reynolds numbers of 800, 1600, 2400 and 3200, respectively.

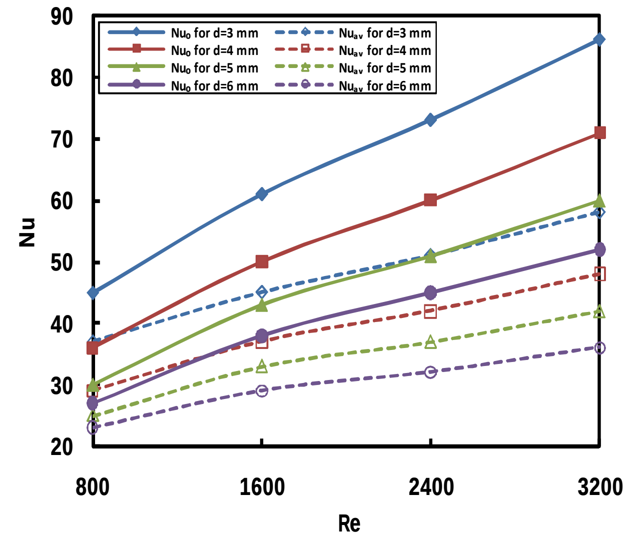

Fig. 6. Variation of Nusselt number with Reynolds number at four different nozzle diameters

Fig. 7 shows the variation of both stagnation and average Nusselt numbers with the Reynolds number for four different nozzle to plate spacings of 4, 5, 6 and 7 (times the nozzle diameter). With the nozzle to plate spacing of 4, the stagnation Nusselt numbers are 39, 54, 64 and 75 besides the average Nusselt numbers of 32, 42, 48 and 55 for the jet Reynolds numbers of 800, 1600, 2400 and 3200, respectively. Likewise, with the nozzle to plate spacing of 5, the stagnation Nusselt numbers are 30, 43, 51 and 60 besides the average Nusselt numbers of 25, 33, 37 and 42 for the jet Reynolds numbers of 800, 1600, 2400 and 3200, respectively. Similarly, with the nozzle to plate spacing of 6, the stagnation Nusselt numbers are 25, 37, 43 and 50 besides the average Nusselt numbers of 21, 28, 32 and 35 for the jet Reynolds numbers of 800, 1600, 2400 and 3200, respectively. Furthermore, with the nozzle to plate spacing of 7, the stagnation Nusselt numbers are 21, 31, 37 and 42 besides the average Nusselt numbers of 18, 24, 27 and 29 for the jet Reynolds numbers of 800, 1600, 2400 and 3200, respectively.

Fig. 8 shows the variation of both stagnation and average Nusselt numbers with the Reynolds number for five different jet inclinations of 30□, 45□, 60□, 75□ and 90□. With the jet inclination of 30□, the stagnation Nusselt numbers are 56, 73, 85 and 98 besides the average Nusselt numbers of 40, 52, 60 and 68 for the jet Reynolds numbers of 800, 1600, 2400 and 3200, respectively. Likewise, with the jet inclination of 45□, the stagnation Nusselt numbers are 46, 62, 73 and 85 besides the average Nusselt numbers of 34, 45, 52 and 59 for the jet Reynolds numbers of 800, 1600, 2400 and 3200, respectively. Similarly, with the jet inclination of 60°, the stagnation Nusselt numbers are 39, 54, 64 and 75 besides the average Nusselt numbers of 29, 39, 45 and 51 for the jet Reynolds numbers of 800, 1600, 2400 and 3200, respectively. Furthermore, with the jet inclination of 75°, the stagnation Nusselt numbers are 34, 48, 57 and 67 besides the average Nusselt numbers of 26, 35, 40 and 46 for the jet Reynolds numbers of 800, 1600, 2400 and 3200, respectively. Additionally, with the jet inclination of 90°, the stagnation Nusselt numbers are 30, 43, 51 and 60 besides the average Nusselt numbers of 25, 33, 37 and 42 for the jet Reynolds numbers of 800, 1600, 2400 and 3200, respectively.

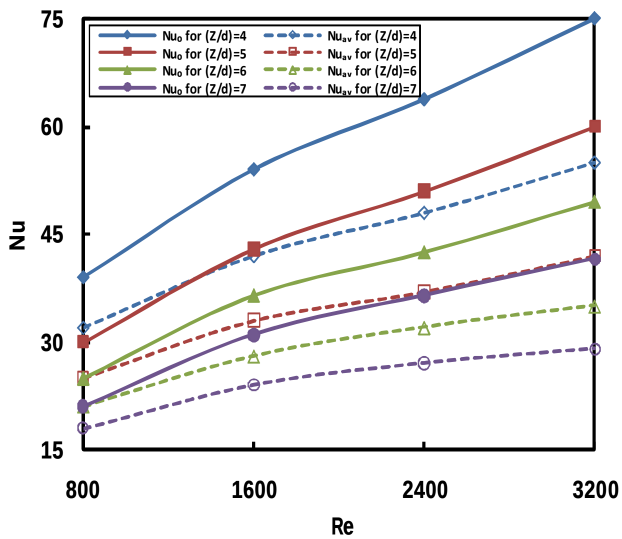

Fig. 7. Variation of Nusselt number with Reynolds number at four different nozzle to plate spacings

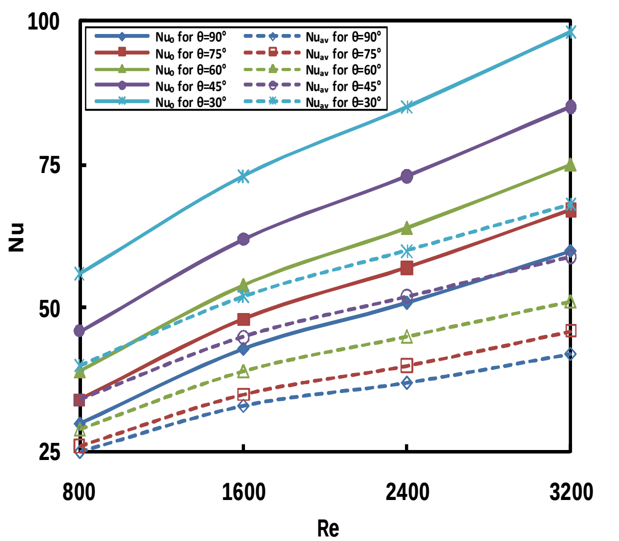

Fig. 8. Variation of Nusselt number with Reynolds number at five different jet inclinations

From the stated figures, it is apparent that both stagnation and average Nusselt numbers increase with jet Reynolds number. It may be due to the fact that the higher jet flow rate (causing the higher jet velocity/jet Reynolds number) results in the taking away of heat from the target plate at faster rate. This result is also expected, from the conventional boundary layer analysis. Furthermore, for a particular Reynolds number, both stagnation and average Nusselt numbers decrease with increase in nozzle diameter (Fig. 6). And also, for a particular Reynolds number, both stagnation and average Nusselt numbers decrease with increase in nozzle-to-target plate spacing/jet inclination (Fig. 7 and Fig. 8). Also, from Figs. 6-8, it is very much clear that the variation of both stagnation and average Nusselt numbers with jet Reynolds number is approximately linear.

VI. CONCLUSION

To study the heat transfer behavior, comprehensive experiments are carried out and accordingly measurements are taken for different combinations of interconnected and interdependent parameters concerned with a water jet impinging on a heated plate. Exhaustive experimental investigations on the effects of the jet Reynolds number and the nozzle diameter are conducted as they highly influence the thermal performance of the water jet impingement. In accordance with the measurements taken and the data obtained, the trends of the results pertaining to various parameters are found to be along expected lines. Besides, the appropriate combinations of the influential and interrelated parameters for which enhancement in the averaged heat transfer from the plate can be expected is also identified. Direct comparison with other experimental/numerical results is not possible due to non-availability of such experimental conditions in the literature. Furthermore, comparison with a numerical model pertaining to the present experimental conditions is planned for the future. In addition, the present study also neglects target plate side heat losses because of lesser thickness comparable to length/breadth. Nevertheless, with the present experimental condition the nozzle diameter of 5 mm with the jet Reynolds number of 2400 gives moderate heat transfer behavior and is the optimum. Hence, the present combination can be used directly in industries to enhance heat transfer and for cooling of electronic systems.

ACKNOWLEDGMENT

The author would like to thank the editor and the reviewers for their kind considerations and precious time along with the painstaking and insightful efforts for reviewing the article.

REFERENCES

[1] S. V. Garimella, B. Nenaydykh. “Nozzle-geometry effects in liquid jet impingement heat transfer” International Journal of Heat and Mass Transfer. 1996; 39(14): pp. 2915–2923.

[2] Roy S, Nasr K, Patel P, Abdul Nour B. “An experimental and numerical study of heat transfer off an inclined surface subject to an impinging airflow” Int J Heat Mass Transfer. 2002; 45(8): pp. 1615–1629.

[3] Chakraborty S, Dutta P. “Analytical solutions for heat transfer during cyclic melting and freezing of a phase change material used in electronic and electrical packaging”. ASME Journal of Electronics Packaging. 2003; 125(1): pp. 126-133.

[4] Lee DH, Song J, Jo MC. “The effects of nozzle diameter on impinging jet heat transfer and fluid flow”. J Heat Transfer. 2004; 126(4): pp. 554-557.

[5] Nayak KC, Saha SK, Srinivasan K, Dutta P. “A numerical model for heat sinks with phase change materials and thermal conductivity enhancers”. Int J Heat Mass Transfer. 2006; 49: pp. 1833-44.

[6] Eren H, Celik N. “Cooling of a heated flat plate by an obliquely impinging slot jet”. Int Comm Heat Mass Transfer. 2006; 33(3): pp. 372–380.

[7] Pavlova A, Amitay M. “Electronic cooling using synthetic jet impingement”. J Heat Transfer. 2006; 128(9): pp. 897-907.

[8] Agostini B, Fabbri M, Park JE, Wojtan L, Thome JR, Michel B. “State of the art of high heat flux cooling technologies”. Heat Transfer Eng. 2007; 28(4): pp. 258–281.

[9] Adoni A, Ambirajan A, Srinivasan K, Dutta P. “Thermo-hydraulic modeling of capillary pumped loop and loop heat pipe”. AIAA Journal of Thermophysics and Heat Transfer. 2007; 21(2): pp. 410-421.

[10] Behera R, Srinivasan K, Dutta P. “Numerical study of interrupted impinging jets for cooling of electronics”. IEEE Transactions Components and Packaging Technologies. 2007; 30(2): pp. 275-84.

[11] Saha SK, Srinivasan K, Dutta P. “Studies on optimum distribution of fins in heat sinks filled with phase change material”. ASME Journal of Heat Transfer. 2008; 130(3): pp. 1-4.

[12] Sagot B, Antonini G, Christgen A, Buron F. “Jet impingement heat transfer on a flat plate at a constant wall temperature”. Int J Thermal Sciences; 47: pp. 1610–1619.

[13] Sanyal A, Srinivasan K, Dutta P. “Numerical study of heat transfer from pin-fin heat sink using steady and pulsated impinging jets”. IEEE Transactions on Components and Packaging Technology. 2009; 32(4): pp. 859-867.

[14] Saha SK, Dutta P. “Heat transfer correlations for PCM-based heat sinks with plate fins”. Applied Thermal Eng. 2010; 30: pp. 2485-2491.

[15] Chaudhari M, Puranik B, Agrawal A. “Heat transfer characteristics of synthetic jet impingement cooling”. Int J Heat Mass Transfer. 2010; 53(5-6): pp. 1057-1069.

[16] Narasimhan A, Reddy BVK, Dutta P. “:Thermal management using the bi-disperse porous medium approach”. Int J Heat Mass Transfer. 2012; 55(4): pp. 538-546.

[17] Yu Z, Xu T, Li J, Ma L, Xu T. “Comparison of a series of double chamber model with various hole angles for enhancing cooling effectiveness”. Int Comm Heat Mass Transfer. 2013; 44: pp. 38–44.

[18] Yu Z, Xu T, Li J, Xiu H, Li Y. “Numerical simulation on the effect of turbulence models on impingement cooling of double chamber model”. Mathematical Problems in Eng. 2013; Article ID 170317: pp. 1-8.

[19] Cheng P, Yao G, Chen W, Li B, Li J, Xu T, Yu Z, Ma L. “Computational study of air/mist impinging jets cooling effectiveness under various curvature models”. Advances in Mechanical Eng. 2014; Article ID 569243: pp. 1-9.

[20] Nguyen T, Liu M, Zhang LC. “Cooling by sub-zero cold air jet in the grinding of a cylindrical component”. Int J Adv Manuf Technol. 2014; 73(1-4): pp. 341-52.

[21] Gould K, Cai SQ, Neft C, Bhunia A. “Liquid jet impingement cooling of a silicon carbide power conversion module for vehicle applications”. IEEE Trans Power Electronics. 2015; 30(6): pp. 2975-2984.

[22] Zhao QY, Chung H, Choi SM, Cho HH. “Effect of guide wall on jet impingement cooling in blade leading edge channel”. J Mech Sci Technol. 2016; 30(2): pp. 525-531.